

Engineering

Industrial & Management Engineering fields

Okayama University

Year 2002

Natural image correction by iterative
projections to eigenspace constructed in
normalized image space

Takeshi Shakunaga
Okayama University

Fumihiko Sakaue
Okayama University

This paper is posted at eScholarship@OUDIR : Okayama University Digital Information
Repository.

<http://escholarship.lib.okayama-u.ac.jp/industrial-engineering/32>

Natural Image Correction by Iterative Projections to Eigenspace Constructed in Normalized Image Space

Takeshi Shakunaga Fumihiko Sakaue
Department of Information Technology
Okayama University
Okayama-shi, Okayama 700-8530, Japan
{shaku,sakaue}@chino.it.okayama-u.ac.jp

Abstract

Image correction is discussed for realizing both effective object recognition and realistic image-based rendering. Three image normalizations are compared in relation with the linear subspaces and eigenspaces, and we conclude that the normalization by L1-norm, which normalizes the total sum of intensities, is the best for our purposes. Based on noise analysis in the normalized image space (NIS), an image correction algorithm is constructed, which is accomplished by iterative projections along with corrections of an image to an eigenspace in NIS. Experimental results show that the proposed method works well for natural images which include various kinds of noise shadows, reflections and occlusions. The proposed method provides a feasible solution to the object recognition based on the illumination cone [2]. The technique can also be extended to face detection of unknown person and registration/recognition using eigenfaces.

1. Introduction

In object recognition, eigenspaces are often constructed in a least-squared sense, faithful to the original images [7]. Eigenspaces are also effective for image based rendering [4, 3]. They can also be constructed from original images based on the photometric SVD algorithm [8]. These methods are commonly discussed in the original image space. Although the original image space is effective for some purposes, it often doesn't work when illumination is out of range. In such a case, we empirically utilize some types of image normalization. We would like to discuss which normalization is rational from a viewpoint of object recognition and photometric analysis.

2. Image Normalization

2.1. Three Definitions of Normalization

Three types of the normalization are used in a variety of image analyses and computer vision. Their definitions and characteristics are summarized as follows.

(1) Normalization by average and variance

A normalization based on the average and variance is often used for object recognition. Although this type of normalization is closed to any averaging operation, some important information is lost when variance is compelled to be a constant. Furthermore, constant images cannot be covered with this normalization.

(2) Normalization by L2-norm

Another normalization based on L2 norm is widely used for object/face recognition. However, this normalization suffers from a problem that the average of a set of "normalized" images is not "normalized".

(3) Normalization by L1-norm

The third normalization is based on L1-norm. Let an N -dimensional vector \mathbf{X} denote an image of which any element is non-negative, and $\mathbf{1}$ denote an N -dimensional vector of which any element is 1. The normalized image \mathbf{x} of an original image \mathbf{X} is defined as $\mathbf{x} = \mathbf{X}/(\mathbf{X}^T \mathbf{1})$. After the normalization, \mathbf{x} is normalized in the sense that $\mathbf{x}^T \mathbf{1} = 1$.

Any nonzero image $\mathbf{X} (\neq \mathbf{0})$ is mapped to a point in the Normalized Image Space (NIS) by this normalization. The NIS is closed to any averaging operation, and the real variance is encoded up to a scale factor.

2.2. NIS as Intensity-Invariant Image Space

In the three normalizations, normalization by L1-norm is very natural in that the total energy is normalized in each image. It also has some advantages

because NIS is closed to averaging operations. This property simplifies the construction and the maintenance of eigenspaces on it. Fundamental properties with NIS are summarized in 2.3 and 2.4. Effect of noise is analyzed in 3.1, and image correction method is discussed in 3.2 and 3.3.

2.3. Linear subspace in NIS

NIS provides an image representation invariant to the light intensity change if the original image doesn't include either saturated points or any shadow regions. This means that the 3D linear subspace for Lambertian surface [6] in the N -dimensional original image space is mapped to a 2D linear subspace in the $(N - 1)$ -dimensional NIS, as shown in Fig. 1.

According to the linear subspace model, any original image \mathbf{X} of Lambertian object can be represented in a linear sum of three images $\mathbf{X}_i (i = 1, 2, 3)$ taken under three independent lighting conditions. We can write the relation as $\mathbf{X} = \sum_i w_i \mathbf{X}_i$, where w_i is a weight parameter. This relation is mapped to a relation in NIS as

$$\mathbf{x} = \sum_{i=1}^3 \frac{w_i (\mathbf{X}_i^T \mathbf{1}) \mathbf{x}_i}{\sum_i w_i (\mathbf{X}_i^T \mathbf{1})}$$

The mapping from the original image space to the NIS is analogous to a mapping from the 3D (R - G - B) color space to the colorimeter plane which is defined by hue and saturation. Replacing (R, G, B) with $(\mathbf{X}_1, \mathbf{X}_2, \mathbf{X}_3)$, we can make the 2D linear subspace which includes $\mathbf{x}_1, \mathbf{x}_2$ and \mathbf{x}_3 , as shown in Fig. 1. The 2D linear subspace can represent a Lambertian object up to an intensity factor when any image includes no shadow regions.

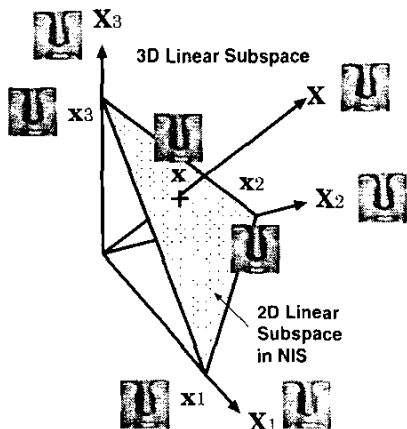


Figure 1. Linear subspace in NIS.

2.4. Eigenspace in NIS

Discussion for the linear subspaces can be applied to that for eigenspaces because they are regarded as orthogonalized linear spaces. In previous work, eigenspaces are often constructed around the origin of image space [8] as same as the linear subspaces when a photometric analysis is essential and inevitable. On the other hand, eigenspaces are often constructed around the average image [7, 1] when the results are used for the recognition based on the subspace method. However, these two types of eigenspaces are converted to each other when the latter type is constructed in NIS.

Eigenspaces in NIS work well for the illumination-independent recognition of non-Lambertian objects when the object shapes can be fixed. For example, 2D face recognition can be reduced to the subspace method using low dimensional eigenspaces in NIS.

3. Noise Detection and Image Correction

3.1. Effect of Noise in NIS

Let us analyze the effect of noise to the projection to eigenspace in NIS and the residual. Suppose that an object view are completely encoded to k dimensional eigenspace by

$$\mathbf{x}^* = \Phi_k^T (\mathbf{x} - \bar{\mathbf{x}})$$

where Φ_k consists of k orthonormal bases of the eigenspace and $\bar{\mathbf{x}}$ denotes the center of the eigenspace.

Let \mathbf{n} and \mathbf{y} denote the normalized images of image \mathbf{N} and $\mathbf{X} + \mathbf{N}$, and $\mathbf{y} = (1 - \alpha)\mathbf{x} + \alpha\mathbf{n}$. Then the projection \mathbf{y}^* and the residual $\mathbf{y}^\# = \mathbf{y} - \bar{\mathbf{x}} - \Phi_k \mathbf{y}^*$ are represented in

$$\mathbf{y}^* = (1 - \alpha)\mathbf{x}^* + \alpha\Phi_k^T (\mathbf{n} - \bar{\mathbf{x}}) \quad (1)$$

$$\mathbf{y}^\# = \alpha\mathbf{n}^\# = \alpha(\mathbf{n} - \bar{\mathbf{x}}) - \alpha\Phi_k \Phi_k^T (\mathbf{n} - \bar{\mathbf{x}}). \quad (2)$$

In Eq. (2), the first term indicates an existence of \mathbf{n} itself. The second term indicates that the noise affects whole the image with weight $-\alpha\Phi_k \Phi_k^T$. Even if \mathbf{n} is very localized, the effect spreads to the whole image. Since $\Phi_k \Phi_k^T$ is positive semi-definite, the second term yields a negative reaction to the noise. In general, negative reaction is generated from positive noise, while positive reaction is generated from negative noise.

3.2. Noise Detection by Relative Residue

Let us define a relative residue r_i for the i -th pixel of \mathbf{x} by

$$r_i = \frac{\mathbf{e}_i^T \mathbf{x}^\#}{\mathbf{e}_i^T (\bar{\mathbf{x}} + \Phi_k \mathbf{x}^*)}$$

where $\mathbf{x}^\# = \mathbf{x} - \bar{\mathbf{x}} - \Phi_k \mathbf{x}^*$ and \mathbf{e}_i is a unit vector which has 1 in the i -th element and 0s in the others. We use the relative residue in spite of absolute residue ($\mathbf{e}_i^T \mathbf{x}^\#$) because we would like to suppress noise not in absolute scale but in relative one. For example, small noise in the dark area had better to be suppressed when the relative residue is big enough.

Noise detection is basically made by $|r_i|$. However, Eq. (2) suggests that the zero level of the relative residue may shift due to the amount of noise and Φ_k when a considerable amount of noise is included. In order to compensate the possible shift, we use $|r_i - \hat{r}|$ in spite of $|r_i|$ where \hat{r} is the median of the whole r_i . We don't use the average because we would like to neglect the direct noise factors in Eq. (2). Consequently, noise can be detected by the relation $|r_i - \hat{r}| \geq r_\theta$, when r_θ is a threshold.

3.3. Image Correction by Projection

The noise correction algorithm can be made based on the noise detection as follows: When $|r_i - \hat{r}| \geq r_\theta$, the i -th pixel of \mathbf{x} should be replaced by $\mathbf{e}_i^T (\bar{\mathbf{x}} + \Phi_k \mathbf{x}^*)$. The image correction makes an intensity value to be consistent with the projection. For example, shadows and reflection regions are corrected.

It is noted that the normality of the image doesn't hold after the correction. Therefore, the corrected image should be re-normalized when all the pixels are checked and corrected.

The projection-based correction just changes outliers to inliers. When not a few pixels are corrected, \mathbf{x}^* also changes to some extent. Therefore, a few iterations of correction should be necessary for better noise suppression. After iterations, \mathbf{x} converges to an image along with little noise or shadow.

3.4. Noise Detection/Correction via Canonical Space

When an eigenspace is constructed from various shapes in an object class, it may not work with a quite different shape because the eigenspace depends on the object shapes. However, the eigenspace still works when the object shapes are statistically stable in the class. For example, the eigenface technique [7] has been widely used for the detection of unknown faces based on the statistic stability of human faces. Recently, [5] proposed face analysis and effective construction of individual eigenfaces using a canonical eigenface constructed from face images of 50 persons in 24 lighting conditions. Given any face image, the image correction algorithm mentioned in 3.3 can be applied

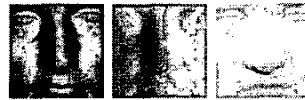


Figure 2. Example of eigenplane for Lambertian surface: Average and 2 principal bases.



Figure 3. Two examples of image correction: In each triplet from left to right, original \mathbf{x} , detected noise region and final result.

without any revision. The image correction improves the discrimination rate [5].

4. Experimental Results and Applications

4.1. Eigenplane for Lambertian Object

As mentioned in 2.4, 2D eigenspace (eigenplane) is constructed for a Lambertian object. An example of eigenplane is as shown in Fig. 2, which is constructed in NIS from ten images of a Napoleon statue made of plaster. In Fig. 2, the left image shows the average image while the others show the two orthonormal bases of the eigenplane.

Two examples of image correction are shown in Fig. 3. In the both examples, the corrections are made around the nose, where the cast shadow regions are detected and corrected by the projection.

4.2. Image Correction with Individual Eigenface

For a non-Lambertian object, the projection-based image correction works well. An example of eigenspace is as shown in Fig. 4, which is constructed in NIS from six individual faces. In Fig. 4, the left image shows the average image while the others show the most significant 3 orthonormal bases of the eigenface.

Three examples of image correction are shown in Fig. 5. In the left two pair, the corrections are made around nose, where the cast shadow regions are detected and corrected by the projection. In the right most example, the correction is made for the artificial occlusion. These examples show that the projection-based image correction is very robust to both shadows and occlusions.

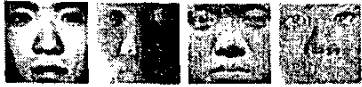


Figure 4. Eigenface for individual: Average and 3 principal bases.

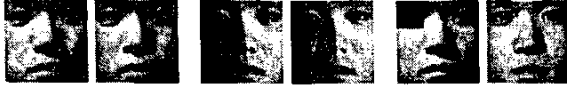


Figure 5. Examples of image correction: In each pair, x is shown in the left and the final result in the right.

4.3. Image Correction with Canonical Eigenface

For a class of human faces, the projection-based image correction still works. A canonical eigenface, as shown in Fig. 6, is constructed in NIS from 50 faces in 20 lighting conditions for each. In Fig. 6, the left image shows the average image while the others show the most significant 5 bases of the eigenface.

We compare the results between 3D and 45D eigenfaces in Fig. 7. In these two examples, similar results are gotten with 3D and with 45D, while x^* is less similar to the x when the 3D eigenface is used. The right example also shows that the image correction works not only for the mirror reflection on his glasses but also for the half-transparent occlusion by his glasses. In this case, glasses are removed in the results because the canonical eigenface doesn't include persons with glasses.

5. Conclusions

The normalized image space (NIS) is very useful in combination with eigenspaces. Eigenspaces in NIS enable us to realize the object recognition, photometric analysis and image correction in the same domain. Experimental results show that the projection-based image correction is very effective for a variety of eigenspaces. The technique can also be applied to object recognition including shadows, reflections and



Figure 6. Canonical eigenface constructed from 50 persons: Average and 5 principal bases.



Figure 7. Two examples of image correction: In each triplet from left to right, original x , result images corrected with 3D and 45D eigenfaces.

occlusions.

Acknowledgment

This work has been partly supported by Japan Science and Technology Corporation under Ikeuchi CREST project.

References

- [1] Belhumeur, P. N., Hespanha, J. P., Kriegman, D. J., "Eigenfaces vs. Fisherfaces: Recognition Using Class Specific Linear Projection", IEEE Trans. PAMI, 19(7), pp.711-720, 1997.
- [2] Georghiades, A. S., Belhumeur, P. N. and Kriegman, D. J., "From few to many: illumination cone models for face recognition under variable lighting and pose", IEEE Trans. PAMI, 23(6), pp.643-660, 2001.
- [3] Mukaigawa, Y., H. Miyaki, S. Mihashi and T. Shakunaga, "Photometric Image-Based Rendering for Image Generation in Arbitrary Illumination," Proc. ICCV2001, vol.2, pp.652-659, 2001.
- [4] Nishino, K., Y. Sato, and K. Ikeuchi, "Eigen-texture method: appearance compression and synthesis based on a 3D model", IEEE Trans. PAMI, 23(11), pp.1257-1265, 2001.
- [5] Shakunaga, T., K. Shigenari, "Decomposed Eigenface for Face Recognition under Various Lighting Conditions," Proc. CVPR2001, vol. 1, pp.864-871, 2001.
- [6] Shashua, A., "Geometry and Photometry in 3D visual recognition", Ph.D. Thesis, MIT, 1992.
- [7] Turk, M. and Pentland, A., "Eigenfaces for Recognition", Journal of Cognitive Neuroscience, vol. 3, no. 1, pp. 71-86, 1991.
- [8] Yuille, A. L., Epstein, S. R. and Belhumeur, P. N., "Determining Generative Models of Objects Under Varying Illumination: Shape and Albedo from Multiple Images Using SVD and Integrability", International Journal of Computer Vision, vol. 35, no.3, pp.203-222, 1999.